GMR
The Original

ECO-FRIENDLY SYNTHESIS OF SELENIUM NANOPARTICLES USING RHODODENDRON EXTRACT AND THEIR ANTIMICROBIAL PROPERTIES

Pratishtha Raturi[1], Neha Rawat[1], Nabeel Ahmad[2]

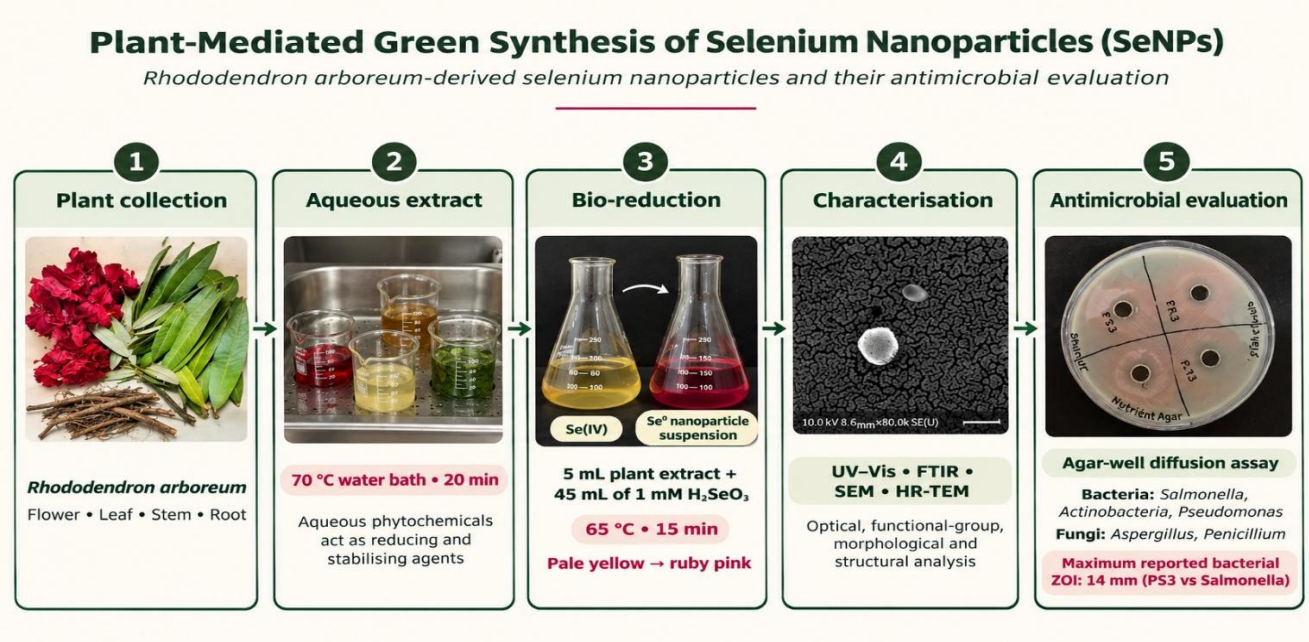
[1]PhD Scholar; Department of Microbiology; School Of Allied Sciences; Dev Bhoomi Uttarakhand University, Dehradun, Uttarakhand
[2]Department of Biotechnology; School Of Allied Sciences; Dev Bhoomi Uttarakhand University, Dehradun; Email: nabeel.biotech@gmail.com

ABSTRACT

The biological utility of selenium nanoparticles (SeNPs) rests on a favorable combination of selenium's nutritional role with the surface chemistry available at nanoscale; nonetheless, their movement into medical applications continues to be hindered by the harsh reagents and high energy requirements typical of solution-phase chemical methods. The work reported here describes an aqueous, phytochemically driven preparation of SeNPs that uses four separately prepared extracts of Rhododendron arboreum — derived from flower, leaf, stem, and root extracts— sampled from a high-altitude population in the Garhwal Himalaya, and benchmarks the resulting batches (designated SeNP-PF, SeNP-PL, SeNP-PR, SeNP-PS) across structural and antimicrobial endpoints. Treatment of 1 mM selenious acid with each extract at 65 °C for 15 min produced a striking transition from pale yellow to ruby pink, a visual signature of Se(IV) reduction. UV–visible spectroscopy located a surface plasmon resonance feature in the 500–550 nm window, with the strongest absorbance under near-neutral conditions; FTIR returned hydroxyl, carbonyl, and C–O bands at ≈3339, 1634, and 1125–1257 cm−1 that are consistent with phenolic-based capping. SEM and TEM observations showed rounded to irregular electron-dense features, with differences in their observed distribution and aggregation among plant-part-derived preparations. In agar-well diffusion screening, stem-derived SeNP-PS produced the largest single inhibition zones against Salmonella sp. (14 mm) and Actinobacteria (13 mm), while flower-derived SeNP-PF was strongest against Pseudomonas sp. (13 mm). We report here a plant-part-resolved evaluation of R. arboreum-mediated SeNP synthesis and biological activity.

KEYWORDS: Selenium nanoparticles, Green synthesis, Rhododendron arboreum, Plant-part comparison, Antimicrobial activity

Graphical Abstract



Five-step depiction of plant-part-differentiated green synthesis and antimicrobial evaluation of selenium nanoparticles from Rhododendron arboreum.

1.Plant collection: Leaves, flowers, roots, and stems were collected from the Garhwal Himalaya.

2.Extract preparation: Aqueous extracts were prepared by heating the plant materials in a water bath at 70 °C.

3.Nanoparticle synthesis: The extracts were reacted with 1 mM H_2SeO_3 at 65 °C for 15 min, accompanied by a yellow-to-ruby colour change.

4.Characterization: UV–Vis, FTIR, and SEM were used to investigate optical properties, functional groups, and particle morphology, respectively.
5.Antibacterial evaluation: Agar-well diffusion testing showed a 14 mm zone of inhibition against Salmonella sp.

1. INTRODUCTION

Selenium (Se) is an essential trace element required for several physiological processes in mammals, primarily through its incorporation into selenoproteins. Among these, glutathione peroxidases and thioredoxin reductases play important roles in maintaining cellular redox balance and protecting cells against oxidative stress. However, the biological effects of selenium are strongly influenced by its chemical form and level of exposure, as the range between nutritional requirement and toxicity is relatively narrow [1–3]. These considerations have encouraged research into alternative selenium formulations that may offer improved physicochemical and biological characteristics.

Selenium nanoparticles (SeNPs) have attracted considerable interest because of their reported antioxidant, antimicrobial and other biological properties. Compared with some conventional inorganic selenium compounds, elemental selenium in nanoparticulate form has demonstrated a potentially favourable toxicity profile in certain experimental systems. Nevertheless, these properties are not universal and may vary with particle size, morphology, surface chemistry, synthesis conditions and administered concentration [4–6]. Consequently, the synthesis route is an important factor in determining the characteristics and subsequent biological behaviour of SeNPs. Although physical and chemical approaches are established methods for nanoparticle production, biological synthesis has gained attention as an alternative that can employ relatively mild reaction conditions and biologically derived materials. In plant-mediated synthesis, naturally occurring constituents such as phenolic compounds, flavonoids, proteins, carbohydrates and other metabolites may participate in selenium precursor reduction and nanoparticle stabilisation. The composition of the plant extract and the reaction parameters can therefore influence nanoparticle formation and the properties of the resulting preparation [4, 7–10].

Among plant-based resources, Rhododendron arboreum, a member of the family Ericaceae, is a medicinal tree widely distributed across the Himalayan region. Different parts of this species have been described in traditional uses and phytochemical investigations, with reports documenting the presence of phenolic compounds, flavonoids and other secondary metabolites [11, 12]. In particular, analytical investigation of R. arboreum flowers has identified a diverse range of anthocyanins, flavonoids and phenolic acids, while studies of flower extracts have also reported antioxidant potential [13, 14, 15]. These findings provide a scientific basis for investigating R. arboreum as a potential plant resource for nanoparticle synthesis. Importantly, the phytochemical composition of a plant may differ among its organs; therefore, flower, leaf, stem and root extracts may not necessarily contribute identical reducing or stabilising constituents during nanoparticle formation. Evaluating these plant parts under a common synthesis protocol may help establish whether plant-part selection is associated with differences in the characteristics and preliminary biological responses of the resulting preparations.

In this context, the present study was designed to synthesise selenium nanoparticle preparations separately using flower, leaf, root and stem extracts of R. arboreum. The resulting preparations were examined using ultraviolet–visible spectroscopy (UV–Vis), Fourier-transform infrared spectroscopy (FTIR), scanning electron microscopy (SEM) and transmission electron microscopy (TEM) to investigate their spectral characteristics, surface-associated functional groups and morphology. Their preliminary antibacterial activity was screened against Salmonella sp., Pseudomonas sp. and Actinobacteria, while antifungal screening was performed against Aspergillus sp. and Penicillium sp. using the agar-well diffusion method. The study therefore aimed to compare preparations obtained from different plant parts within a common experimental framework and to explore the potential influence of plant-part selection on their physicochemical characteristics and preliminary antimicrobial observations.

2. MATERIALS AND METHODS

2.1 Plant material and extract preparation

Disease-free flowers, leaves, stems and roots of R. arboreum were collected from cultivated/research-station stock at Rani-chauri (Tehri Garhwal district, Uttarakhand, India; high-altitude Himalayan provenance). No animal subjects were involved at any stage of the work. Each plant part was first rinsed under running tap water and subsequently with distilled water, allowed to air-dry at room temperature, and then chopped finely with a sterile scalpel. Ten grams of the chopped material was transferred to 100 mL of distilled water in a 250 mL borosilicate beaker and heated in a water bath at 70 °C for 20 min. After cooling to room temperature, the mixture was filtered through Whatman No. 1 filter paper. The four resulting aqueous extracts — designated PF (flower extract), PL (leaf extract), PR (root extract) and PS (stem extract) — were stored at 4 °C until further use.

2.2 SeNP biosynthesis

SeNPs were synthesised using the aqueous extracts of R. arboreum. An aqueous solution of 1 mM selenious acid (H_2SeO_3) was prepared using distilled water. For each synthesis reaction, 5 mL of the respective plant extract was added to 45 mL of the selenious acid (H_2SeO_3, 98%, Sigma-Aldrich) solution in a conical flask.

The reaction mixture was maintained at 65 °C under continuous magnetic stirring for 15 min. The progress of the reaction was monitored visually through a colour change from pale yellow to ruby pink, indicating the formation of selenium-containing nanoparticulate material. The resulting preparations were designated as SeNP-PF, SeNP-PL, SeNP-PR and SeNP-PS, corresponding to flower, leaf, root and stem extracts, respectively [4].

2.3 Reaction-parameter optimization

2.3.1 Effect of pH

The influence of reaction pH on selenium nanoparticle formation was investigated over a range of pH 4–9. The pH of the reaction mixtures was adjusted using 0.1 M hydrochloric acid (HCl) or 0.1 M sodium hydroxide (NaOH). The mixtures were incubated at 60 °C under continuous stirring for 2 h. Following incubation, the samples were analysed using UV–visible spectroscopy over the wavelength range of 300–800 nm to evaluate their absorption characteristics.

2.3.2 UV–Visible Monitoring of Temperature- and Time-Dependent Changes

A separate temperature- and time-dependent investigation was performed at 10, 20, 30, 40 and 50 °C. The changes in UV–visible absorbance were monitored at hourly intervals over a period of 1–6 h to assess the progression of nanoparticle formation. The experiments were performed in triplicate, and the recorded absorbance values were expressed as means.

2.4 Physicochemical Characterisation

2.4.1 UV–Visible Spectroscopy

The optical characteristics of the synthesised SeNP preparations were investigated using a UV–visible spectrophotometer over the wavelength range of 200–800 nm. The absorption profiles were examined to identify characteristic absorption features associated with nanoparticle formation and to compare the optical responses of the different plant-part-derived preparations.

2.4.2 Fourier Transform Infrared Spectroscopy

Fourier transform infrared (FTIR) spectroscopy was employed to investigate the functional groups associated with the synthesised SeNP preparations. The dried samples were mixed with potassium bromide (KBr) and prepared as pellets for spectral analysis. The spectra were recorded over the range of 4000–400 cm^{-1}. The absorption bands were examined to identify possible functional groups associated with the reduction and surface stabilisation of the nanoparticles.

2.4.3 Scanning Electron Microscopy

The surface morphology of the synthesised SeNP preparations was examined using scanning electron microscopy (SEM). The samples were subjected to sputter coating before imaging to improve surface conductivity. The micrographs were examined to assess the morphological and surface characteristics of the nanoparticle preparations.

2.4.4 High-Resolution Transmission Electron Microscopy

The synthesised nanoparticle preparations were purified by repeated centrifugation at 12,000 rpm for 20 min, followed by washing with deionised water. The purified material was dispersed by ultrasonication, and a 5 µL aliquot was deposited onto a carbon-coated copper grid and allowed to air-dry at room temperature.

HR-TEM analysis was performed at an accelerating voltage of 200 kV to examine particle morphology and structural characteristics. HR-TEM imaging was performed to examine the morphology and distribution of electron-dense structures in the preparations.

2.5 Antibacterial assay

Antibacterial activity of the synthesised selenium nanoparticle (SeNP) preparations was evaluated using the agar-well diffusion method against three bacterial test organisms: Salmonella sp., Pseudomonas sp. and an actinobacterial isolate. The organisms were obtained as clinical isolates from a clinical laboratory in Dehradun, India.

Nutrient agar plates were uniformly inoculated with the respective bacterial cultures. Wells were prepared using a sterile cork-borer, and 50 µL of the corresponding SeNP suspension was added to each well. The plates were incubated at 37 °C for 24 h. Following incubation, the zones of inhibition (ZOI) were measured in millimetres using a digital caliper [16].

2.6 Antifungal assay

Antifungal activity of the synthesised SeNP preparations was evaluated against Aspergillus sp. and Penicillium sp., obtained as clinical isolates from a clinical laboratory in Dehradun, India.

The agar-well diffusion assay was performed using potato dextrose agar (PDA) plates inoculated with the respective fungal cultures. Wells were prepared in the agar medium and loaded with 50 µL of the corresponding SeNP suspension. The plates were incubated at 25 °C for 48 h. Following incubation, the presence or absence of visible inhibition zones was recorded, and detectable zones were measured in millimeters [16,17].

2.7 Statistical analysis

Temperature-optimisation absorbance values are reported as means of three independent runs. Antibacterial and antifungal zone-of-inhibition measurements were recorded as single observations per well per organism (n = 1).

3. RESULTS AND DISCUSSION

3.1 Biosynthesis of SeNPs

The addition of aqueous Rhododendron arboreum extracts to 1 mM selenious acid (H_2SeO_3), followed by incubation at 65 °C under continuous stirring, resulted in a visible colour change from pale yellow to ruby pink within 15 min. This colour transition was considered a preliminary indication of selenium-containing nanoparticulate material formation and may be associated with the reduction of Se(IV) by plant-derived constituents. A similar colour change was observed in all four reaction mixtures prepared using flower, leaf, root and stem extracts, suggesting that extracts from each plant part contained constituents capable of participating in the synthesis process [4]. Plant materials used for extract preparation and the resulting reaction preparations are presented in Fig. 1. The observed colour change was subsequently examined alongside the spectroscopic and microscopic characterisation results.



Fig. 1. R. arboreum plant material used in this study (flowers, left; leaves, right) prior to extract preparation. Material was collected from Rani-chauri, Tehri Garhwal, Uttarakhand, India (high-altitude Himalayan provenance).

3.2 UV–visible spectroscopy

3.2.1 Effect of pH on selenium nanoparticle synthesis

The influence of solution pH on SeNP synthesis was examined over the range pH 4–9 (Fig. 2a). A broad absorption band was observed within the 500–550 nm region, with the highest absorbance recorded at pH 7 (1.25 a.u. at 550 nm). The tabulated measurements showed an increase in peak absorbance from 0.40 a.u. at pH 4 to 0.70, 0.97 and 1.25 a.u. at pH 5, 6 and 7, respectively. Absorbance then decreased to 1.07 a.u. at pH 8 and 0.59 a.u. at pH 9. The relatively stronger response around pH 6–8, particularly at pH 7, suggests that near-neutral conditions favoured the reaction under the conditions tested. This trend may reflect pH-dependent changes in the ionisation and reducing behaviour of plant-derived constituents, which can influence selenium reduction and nanoparticle formation. As the pH series was measured once per condition, these values are descriptive and should not be interpreted as replicated statistical comparisons [4].

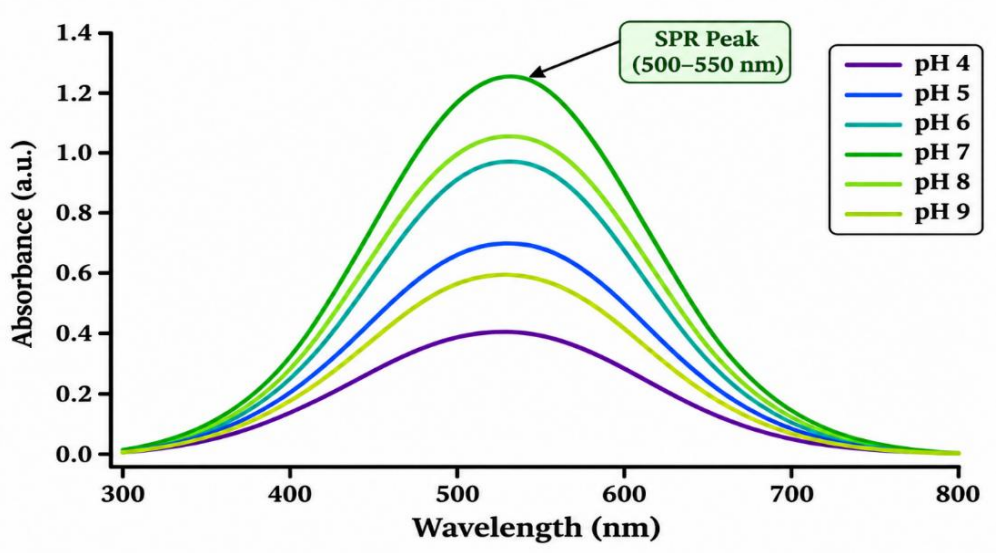


Fig. 2a. Effect of solution pH (4–9) on the UV–visible absorbance spectrum of the SeNP reaction mixture. The shaded region marks the SPR band (500–550 nm). Maximum absorbance was obtained at pH 7.

3.2.2 Effect of reaction temperature on selenium nanoparticle synthesis

The effect of reaction temperature was assessed at 10, 20, 30, 40 and 50°C over 1–6 h by monitoring absorbance at the SPR band (Fig. 2b). Absorbance increased with reaction time at every temperature, and the higher-temperature treatments consistently showed stronger responses. After 6 h, the recorded absorbance values were 0.42, 0.455, 0.545, 0.67 and 0.76 a.u. at 10, 20, 30, 40 and 50 °C, respectively. The maximum value of 0.76 a.u. was therefore observed at 50 °C after 6 h, while the lowest value was recorded at 10 °C. The progressive increase is consistent with faster reaction progression at higher temperatures, potentially because increased thermal energy promotes reduction and nucleation processes. Within the temperature and time ranges examined, 50 °C produced the strongest absorbance response [4,18].

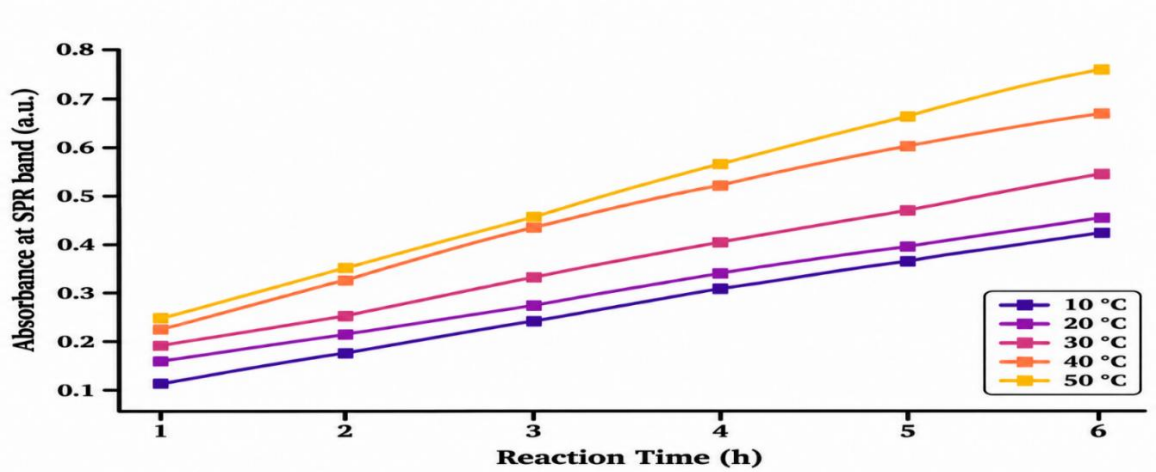


Fig. 2b. Effect of reaction temperature (10–50 °C) on absorbance at the SPR band as a function of time (1–6 h). Data are means of three independent runs.

3.2.3 UV–visible absorption profiles of individual Rhododendron extracts

UV–Visible spectroscopic analysis was performed to examine the absorption characteristics of the flower, leaf, root and stem extracts of Rhododendron (Fig. 2c). The flower extract (PF) exhibited reported absorption maxima at 215.01, 230.01, 244.99, 259.99, 270.00, 294.99, 320.01 and 335.00 nm. Similarly, the leaf extract (PL) showed absorption features at 215.01, 224.99, 244.99, 255.02, 275.00, 285.00, 300.01 and 340.01 nm. In comparison, the root extract (PR) displayed two prominent reported absorption maxima at 224.99 and 235.00 nm, while the stem extract (PS) showed absorption features at 209.98 and 224.99 nm. The differences in the recorded absorption profiles indicate variations in the UV-absorbing constituents among the different plant parts. These constituents may include phytochemicals containing aromatic and conjugated molecular structures. Such compounds may contribute to the plant extracts' potential role as reducing and stabilising agents during the green synthesis of selenium nanoparticles. Further analysis of the synthesised nanoparticles is required to establish changes in their optical properties following the synthesis process.

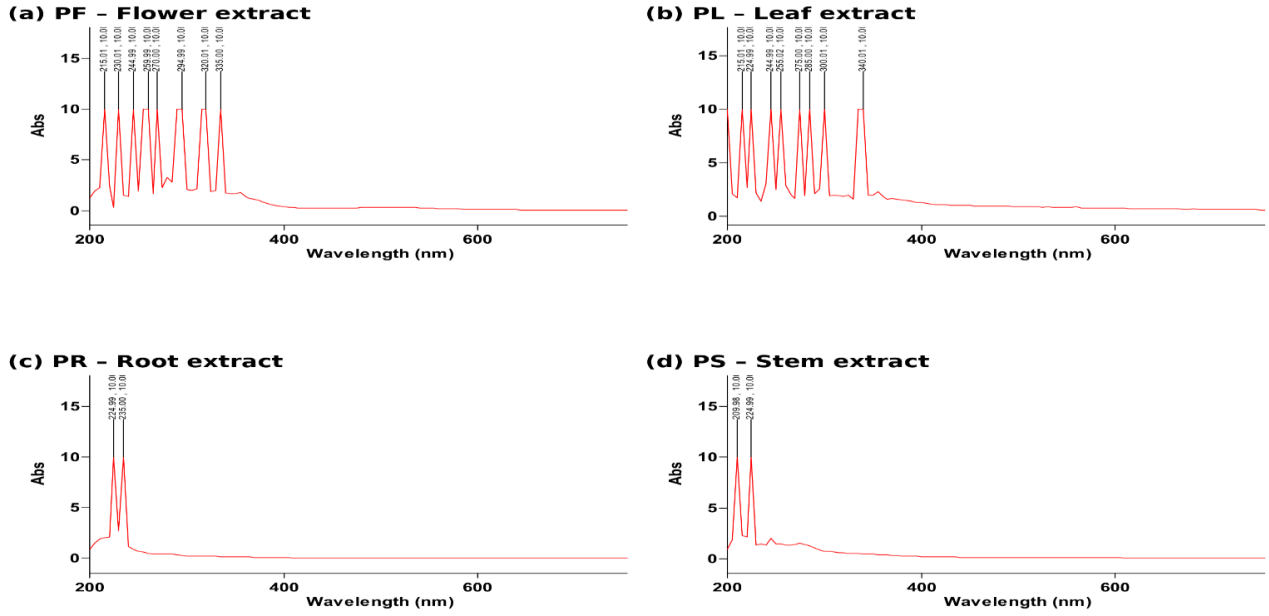


Fig. 2(c). UV–visible absorption spectra of aqueous R. arboreum extracts: (a) flower (PF), (b) leaf (PL), (c) root (PR), and (d) stem (PS).

3.3 FTIR analysis

The FTIR spectra of the lyophilised selenium nanoparticle (SeNP) preparations obtained using the four Rhododendron arboreum extracts (PF, PL, PR and PS) are presented in Fig. 3(a–d). All four spectra exhibited three prominent absorption features at approximately 3339.5, 1634.7 and 1153.9 cm^{-1}. The broad band around 3339.5 cm^{-1} is associated with O–H stretching vibrations of hydrogen-bonded hydroxyl groups, while the band at 1634.7 cm^{-1} may be attributed to carbonyl-containing or conjugated functional groups. The absorption feature near 1153.9 cm^{-1} is consistent with C–O stretching vibrations associated with alcohol, ether and glycosidic groups [19]. Additionally, the root-derived SeNP preparation (PR) exhibited bands at approximately 1198.9 and 1257.9 cm^{-1}, whereas the stem-derived preparation (PS) showed an additional feature at 1198.9 cm^{-1}. These variations in the fingerprint region may reflect differences in the functional-group composition of the respective plant extracts. The presence of hydroxyl-, carbonyl- and C–O-associated absorption bands suggests the involvement of plant-derived phytochemicals in the reduction and surface stabilisation of SeNPs [4,9]. Overall, the similarities in the major absorption bands indicate the participation of comparable classes of functional groups across all four plant-part preparations, while the additional fingerprint-region features suggest some variation in their phytochemical composition.

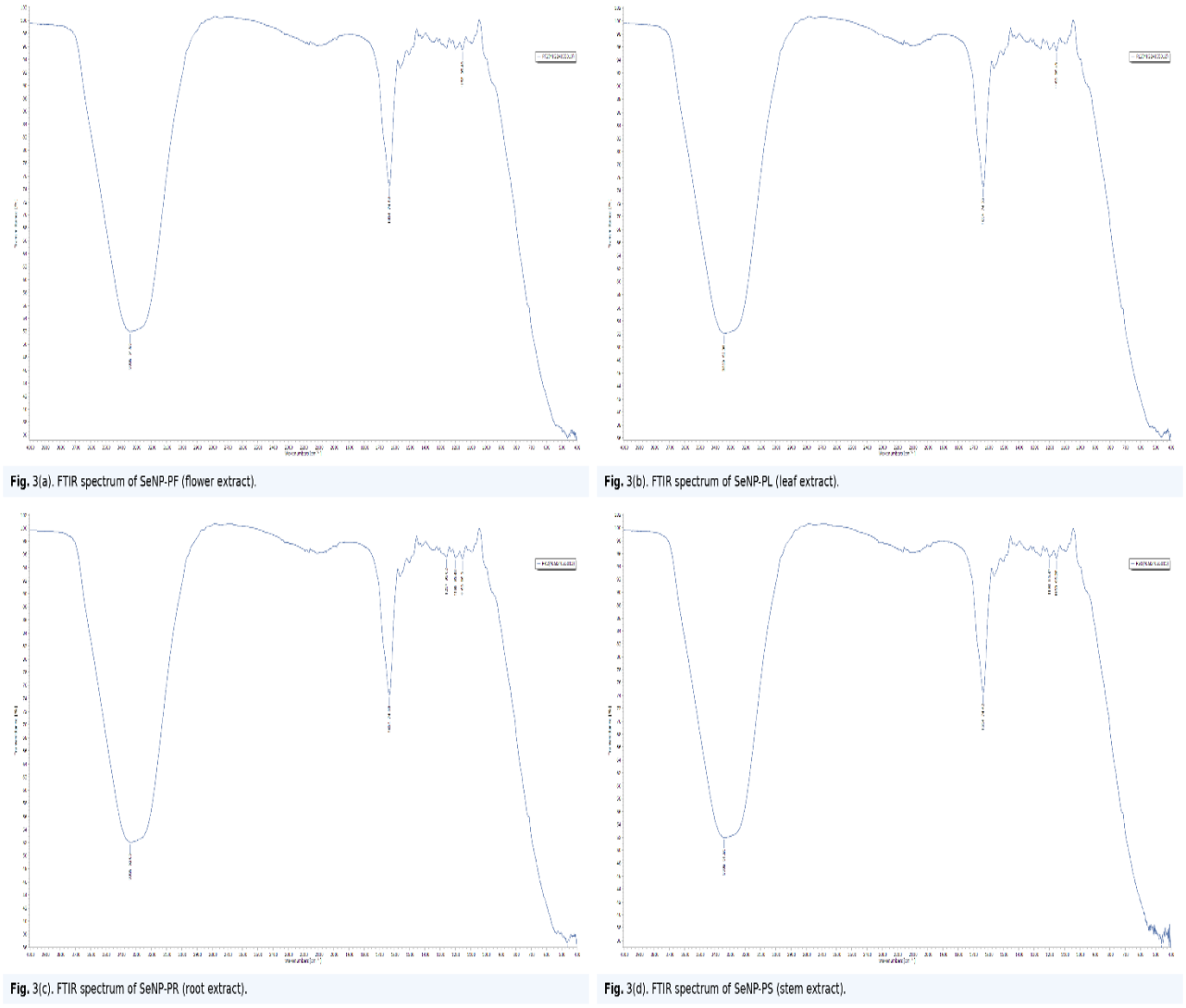


Fig. 3. FTIR spectra of selenium nanoparticles synthesised using different plant parts of Rhododendron arboreum: (a) Flower-derived SeNP-PF, (b) Leaf-derived SeNP-PL, (c) Root-derived SeNP-PR, and (d) Stem-derived SeNP-PS

3.4 SEM morphology

SEM micrographs (Fig. 4) revealed predominantly rounded to approximately spherical particle morphologies in the selenium nanoparticle preparations synthesised using Rhododendron arboreum leaf, flower, root and stem extracts [4]. The leaf-derived sample (Fig. 4a) exhibited an isolated, rounded particle with a clearly distinguishable boundary against the surrounding substrate. The flower-derived sample (Fig. 4b) showed two spatially separated, approximately spherical particles on a textured background. Similarly, the root-derived sample (Fig. 4c) displayed a prominent circular particle accompanied by a smaller particle in the same field. The stem-derived sample (Fig. 4d) also exhibited a distinct rounded particle with a relatively well-defined surface boundary. Overall, the micrographs indicate the formation of rounded SeNP-like structures across all four plant-part preparations, with variations in their observed distribution and surrounding surface features [9,20].

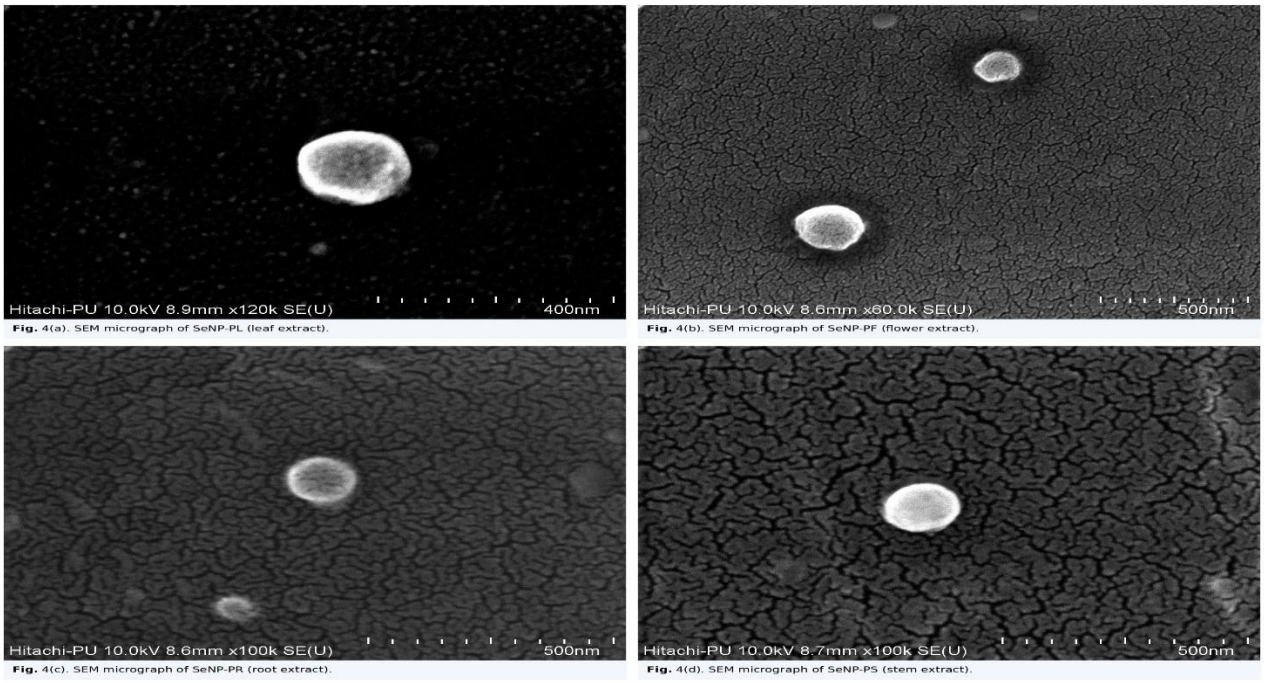


Fig. 4. SEM micrographs showing the surface morphology of selenium nanoparticles synthesised using different parts of Rhododendron arboreum. The micrographs illustrate the rounded particle morphology and surface features of the respective preparations. Scale bars: (a) 400 nm; (b–d) 500 nm.

3.5 High-Resolution Transmission Electron Microscopy (HR-TEM)

High resolution Transmission electron microscopy was performed to investigate the morphology and structural characteristics of selenium nanoparticles synthesised using different plant parts of Rhododendron [18]. The representative micrographs (Figure 5) revealed electron-dense features with predominantly rounded to irregular appearances in all four preparations. The flower-derived sample (SeNP-PF) showed distinguishable particles along with some clustered structures. The leaf-derived sample (SeNP-PL) exhibited rounded features with variations in particle distribution. The root-derived sample (SeNP-PR) displayed distinguishable electron-dense structures with relatively rounded appearances, whereas the stem-derived sample (SeNP-PS) showed multiple small electron-dense features in the selected field [9,21]. Differences in the observed distribution and aggregation patterns were apparent among the plant-part-derived preparations. These morphological observations suggest that the plant extract used during synthesis may influence the appearance and distribution of the resulting nanomaterials. However, further calibrated particle-size measurements and elemental analysis are required to establish their size distribution and confirm their composition.

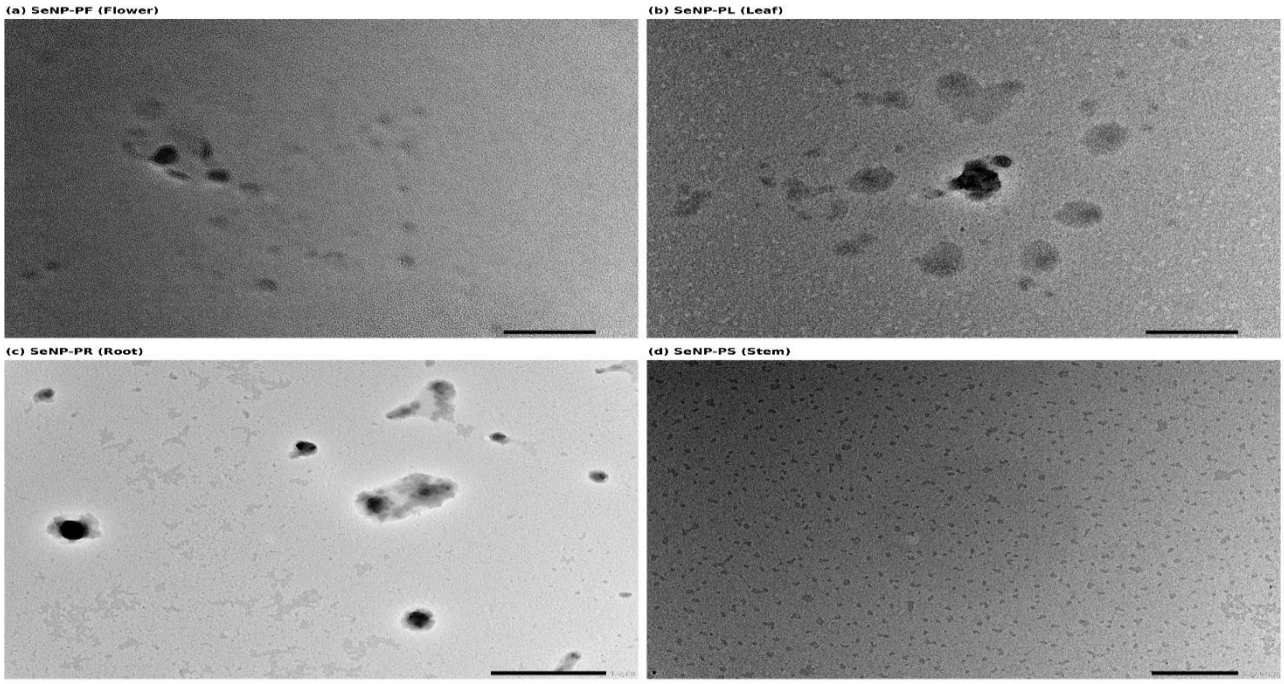


Fig. 5. HR-TEM micrographs of biosynthesized selenium nanoparticles (SeNPs) from four different samples (PF, PL, PR, PS) showing nanoscale particle formation, morphology, distribution, and aggregation behaviour at various magnifications

3.6 Antibacterial activity

Antibacterial activity of the four SeNP preparations against the three test organisms is summarised in Table 1 and Fig. 6. Across the twelve SeNP–organism combinations, ZOI values fell within an 11–14 mm range [22]. The largest single value was 14 mm for SeNP-PS against Salmonella sp., followed by 13 mm values for SeNP-PS against Actinobacteria, for SeNP-PR against Salmonella sp., and for SeNP-PF against Pseudomonas sp. Stem-derived SeNPs (SeNP-PS) produced the largest single observations for two of the three organisms, with flower-derived SeNPs (SeNP-PF) leading against Pseudomonas sp. [20]. The directionality of the differences is consistent with the broader literature view that capping-layer phytochemistry varies across plant parts and tunes the antibacterial response of the resulting SeNPs [23,24].

Table 1. Zones of inhibition (mm) of SeNP preparations against test bacteria by agar-well diffusion (50 µL of SeNP suspension per well).

Organism	SeNP-PF	SeNP-PS	SeNP-PR	SeNP-PL
Salmonella sp.	12	14	13	12
Actinobacteria	11	13	12	12
Pseudomonas sp.	13	11	12	11

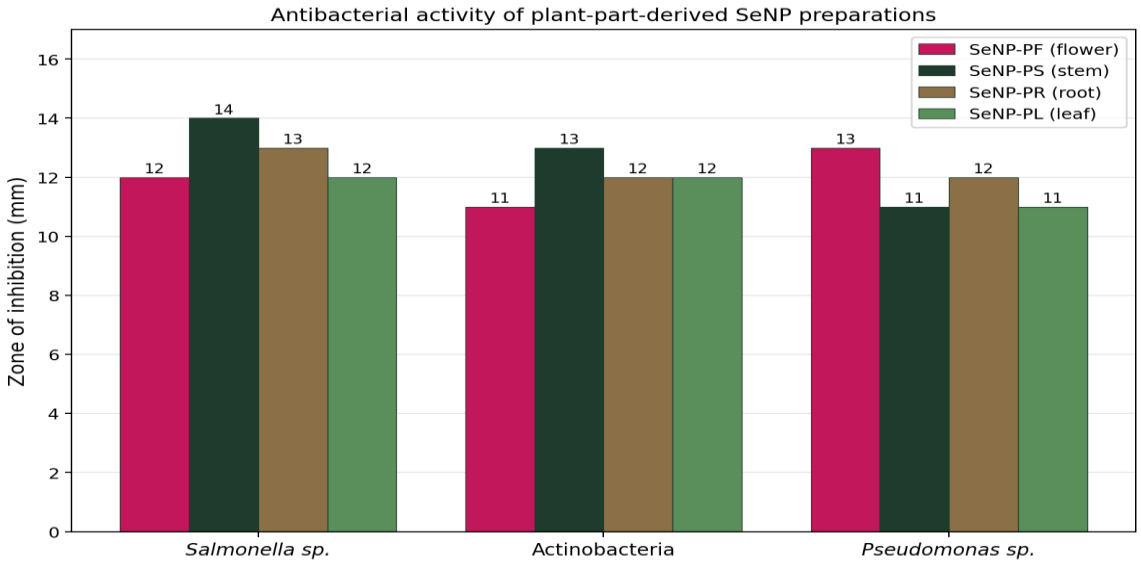


Fig. 6. Antibacterial zones of inhibition (mm) of SeNP preparations from each of the four R. arboreum plant-part extracts against Salmonella sp., Actinobacteria, and Pseudomonas sp. by agar-well diffusion.



Fig. 7(a). Representative agar-well diffusion plate against Salmonella sp. Wells are loaded with SeNP-PF, SeNP-PS, SeNP-PR and SeNP-PL.

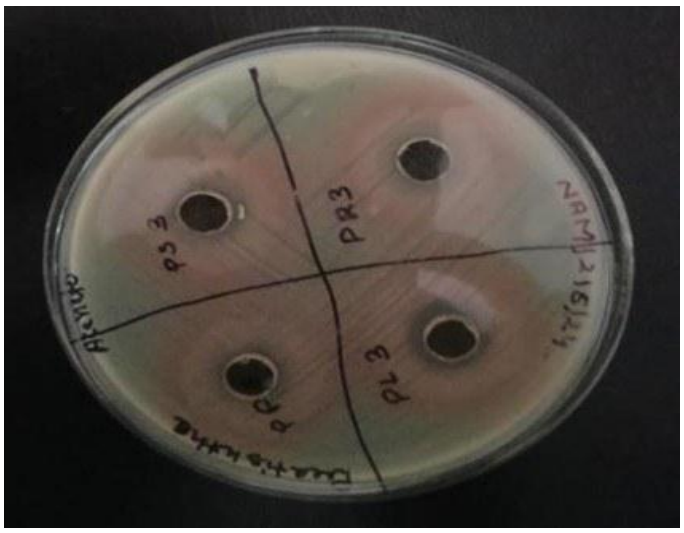


Fig. 7(b). Agar-well diffusion plate against Actinobacteria.

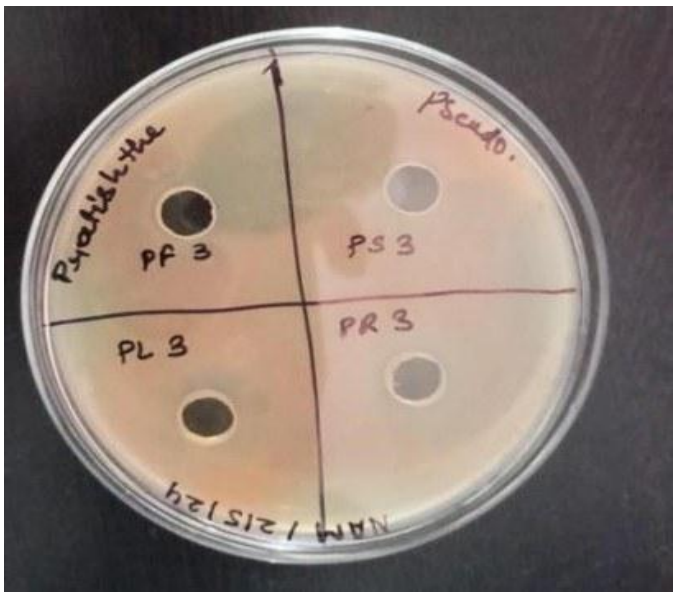


Fig. 7(c). Agar-well diffusion plate against Pseudomonas sp.

3.7 Antifungal activity

Antifungal screening (Table 2 and Fig. 8) returned a sparser and more selective pattern than the antibacterial assay. Against Aspergillus sp., only SeNP-PR produced a visible zone (10 mm); the other three preparations gave no detectable inhibition. Against Penicillium sp., SeNP-PF (11 mm) and SeNP-PL (10 mm) gave detectable zones while SeNP-PS and SeNP-PR did not. Notably, SeNP-PS — the strongest antibacterial preparation against two of three bacteria — showed no antifungal activity against either fungus. This selectivity between bacterial and fungal targets is plausibly attributable to differences between bacterial and fungal cell envelopes, the latter incorporating a more complex chitin-based cell wall that may be less penetrable by the surface chemistry carried by stem-derived SeNPs [25].

Table 2. Zones of inhibition (mm) of SeNP preparations against test fungi by agar-well diffusion. "nil" denotes no detectable inhibition zone.

Organism	SeNP-PF	SeNP-PS	SeNP-PR	SeNP-PL
Penicillium sp.	11	Nil	Nil	10
Aspergillus sp.	Nil	Nil	10	Nil

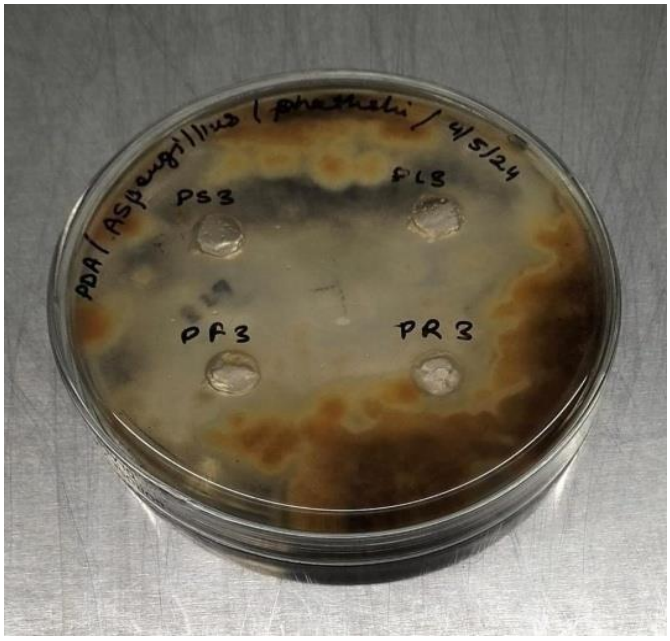


Fig. 8(a). Antifungal plate: Aspergillus sp. on PDA. The zone of inhibition adjacent to the SeNP-PR well is indicated.



Fig. 8(b). Antifungal plate: Penicillium sp. on PDA. Inhibition zones are visible adjacent to the SeNP-PF and SeNP-PL wells.

4 CONCLUSION

This study presents a plant-part-resolved comparison of selenium nanoparticles biosynthesised from R. arboreum flower, leaf, root, and stem aqueous extracts under a single, common reaction protocol. The four preparations yielded morphologically similar approximately spherical particles in the 45–90 nm range, with broadly similar FTIR signatures pointing to polyphenol-based surface capping. UV–visible spectroscopy confirmed an SPR band at 500–550 nm, and optimal synthesis kinetics were obtained at pH 7 and 50 °C within the windows examined. Stem-derived SeNP-PS produced the largest antibacterial zones against Salmonella sp. (14 mm) and Actinobacteria (13 mm), while flower-derived SeNP-PF was strongest against Pseudomonas sp. (13 mm); antifungal activity was selectively concentrated in root- and flower-derived preparations. The plant-part-differentiated approach demonstrated here offers a practical route for tuning the biological activity of plant-mediated SeNPs by selection of source tissue, and supports further development of R. arboreum-derived SeNPs as an environmentally tractable platform for antimicrobial nanomaterials.

5 DECLARATIONS

Funding

The authors received no specific funding for this work.

Conflict of interest

The authors declare no conflict of interest.

Ethical approval

Not applicable — this study did not involve human or animal subjects. Plant material was sourced from cultivated/research-station stock; no Forest Department or institutional ethics clearance was required for collection.

REFERENCES

1. Rayman, M. P. (2012). Selenium and human health. The lancet, 379(9822), 1256-1268.
2. Avery, J. C., & Hoffmann, P. R. (2018). Selenium, selenoproteins, and immunity. Nutrients, 10(9), 1203.
3. Garza-García, J. J., Hernández-Díaz, J. A., Zamudio-Ojeda, A., León-Morales, J. M., Guerrero-Guzmán, A., Sánchez-Chiprés, D. R., ... & García-Morales, S. (2022). The role of selenium nanoparticles in agriculture and food technology. Biological trace element research, 200(5), 2528-2548.
4. Pyrzynska, K., & Sentkowska, A. (2022). Biosynthesis of selenium nanoparticles using plant extracts. Journal of Nanostructure in Chemistry, 12(4), 467-480.
5. Mikhailova, E. O. (2023). Selenium nanoparticles: green synthesis and biomedical application. Molecules, 28(24), 8125.
6. Sampath, S., Sunderam, V., Manjusha, M., Dlamini, Z., & Lawrance, A. V. (2024). Selenium nanoparticles: a comprehensive examination of synthesis techniques and their diverse applications in medical research and toxicology studies. Molecules, 29(4), 801.
7. Fardsadegh, B., Vaghari, H., Mohammad-Jafari, R., Najian, Y., & Jafarizadeh-Malmiri, H. (2019). Biosynthesis, characterization and antimicrobial activities assessment of fabricated selenium nanoparticles using Pelargonium zonale leaf extract. Green Processing and synthesis, 8(1), 191-198.
8. Wadhwani, S. A., Shedbalkar, U. U., Singh, R., & Chopade, B. A. (2016). Biogenic selenium nanoparticles: current status and future prospects. Applied microbiology and biotechnology, 100(6), 2555-2566.
9. Husen, A., & Siddiqi, K. S. (2014). Plants and microbes assisted selenium nanoparticles: characterization and application. Journal of nanobiotechnology, 12(1), 28.
10. Ahmad, N., Bhatnagar, S., Ali, S. S., & Dutta, R. (2015). Phytofabrication of bioinduced silver nanoparticles for biomedical applications. International journal of nanomedicine, 7019-7030.
11. Madhvi, S. K., Sharma, M., Iqbal, J., & Younis, M. (2019). Phytochemistry, traditional uses and pharmacology of Rhododendron arboreum: a review. Research Journal of Pharmacy and Technology, 12(9), 4565-4574.
12. Bisht, A. S. (2024). Rhododendron arboreum: A Valuable medicinal tree from Garhwal Himalaya, Uttarakhand India. International Journal of Bioresource Science, 11(2), 205-209.
13. Bhatt, V., Sendri, N., Swati, K., Devidas, S. B., & Bhandari, P. (2022). Identification and quantification of anthocyanins, flavonoids, and phenolic acids in flowers of Rhododendron arboreum and evaluation of their antioxidant potential. Journal of Separation Science, 45(14), 2555-2565.
14. Jha, A. K., Khalid, M. A., & Labh, S. N. (2024). In vitro antioxidant and antibacterial activities of medicinal flower Laligurans Rhododendron arboreum collected from Kathmandu Valley, Nepal. International Journal of Food Science, 2024(1), 6073042.
15. Painuli, S., Joshi, S., Bhardwaj, A., Meena, R., Misra, K., Rai, N., & Kumar, N. (2018). In vitro antioxidant and anticancer activities of leaf extracts of Rhododendron arboreum and Rhododendron campanulatum from Uttarakhand region of India. Pharmacognosy Magazine, 14(57), 294-294.
16. Balouiri, M., Sadiki, M., & Ibnsouda, S. K. (2016). Methods for in vitro evaluating antimicrobial activity: A review. Journal of pharmaceutical analysis, 6(2), 71-79.
17. Gupta, A., Singh, M., Tiwari, N., Singh, A. P., Shanker, K., Sekar, K. C., & Srivastava, P. K. (2024). Characterization, quantitation, and natural variability of phenolics in Rhododendron arboreum leaves of western Himalayan origin using UPLC-PDA and UHPLC-ESI-Q/TOF-MS/MS. Industrial Crops and Products, 222, 119602.
18. Alsafran, M., Razavi, M. M., Rizwan, M., & Usman, K. (2025). A review on synthesis and characterization of selenium nanoparticles from plant extracts for applications in agriculture, biomedicine, and environment. Green Chemistry Letters and Reviews, 18(1), 2488237.
19. Coates, J. (2000). Interpretation of infrared spectra, a practical approach. Encyclopedia of analytical chemistry, 12, 10815-10837.
20. Gunti, L., Dass, R. S., & Kalagatur, N. K. (2019). Phytofabrication of selenium nanoparticles from Emblica officinalis fruit extract and exploring its biopotential applications: antioxidant, antimicrobial, and biocompatibility. Frontiers in microbiology, 10, 931.
21. Prasad, K. S., & Selvaraj, K. (2014). Biogenic Synthesis of Selenium Nanoparticles and Their Effect on As (III)-Induced Toxicity on Human Lymphocytes: Prasad and Selvaraj. Biological trace element research, 157(3), 275-283.
22. Serov, D. A., Khabatova, V. V., Vodeneev, V., Li, R., & Gudkov, S. V. (2023). A review of the antibacterial, fungicidal and antiviral properties of selenium nanoparticles. Materials, 16(15), 5363.
23. Saleh, A., El-Masry, T. A., Negm, W. A., Alotaibi, B., Elharty, M. E., Alotaibi, K. N., & Elekhnawy, E. (2023). Unravelling the antibacterial potential of biosynthesized selenium nanoparticles against Salmonella Typhimurium food pathogen: in vitro and in vivo investigation. European Review for Medical & Pharmacological Sciences, 27(8), 3631.
24. Zeraatkar, S., Tahan, M., Sadeghian, H., Nazari, R., Behmadi, M., & Hosseini Bafghi, M. (2023). Effect of biosynthesized selenium nanoparticles using nepeta extract against multidrug-resistant Pseudomonas aeruginosa and Acinetobacter baumannii. Journal of Basic Microbiology, 63(2), 210-222.
25. Gow, N. A., & Lenardon, M. D. (2023). Architecture of the dynamic fungal cell wall. Nature Reviews Microbiology, 21(4), 248-259.